2015 European Control Conference (ECC)
July 15-17, 2015. Linz, Austria

On zero-vibration signal shapers and a wave-absorbing controller for a chain of multi-agent dynamical systems

Dan Martinec, Martin Hromčík, Ivo Herman, Tomáš Vyhlídal and Michael Šebek

Abstract— **The paper brings together two different approaches for control of chain of oscillatory lumped-parameter multi-agent systems. Namely, the multi-mode zero-vibration input shaper and the wave-absorbing controller are recalled and the similarities and links between them are broadly discussed. The special case of identical agents with a double-integrator character is at the focus throughout the paper. The report reveals that the two approaches are closely related in spite of the fact that they differ significantly in all aspects, from motivation through computational algorithms to target implementation. In addition, the presented numerical results, mostly based on numerical simulations at this moment, show that the two methods can be combined together, to take advantage of both an appropriate initial excitation of the system by the input shaper and of increased robustness coming from the wave-absorber feedback architecture. Such a combined control law is based on a special property of the multi-mode zero vibration input shaper - namely the convergence of its impulse response, as the number of agents increases, to a double bell-shaped function.**

I. INTRODUCTION

Multi-agent lumped-parameter dynamical systems can be found in many applications and contexts. They can represent multi-body mechanical systems, finite-element models of flexible structures [1], spatially-discretized models of long electrical transmission lines [2], or vehicular platoons [3], [4] and [5]. Most of the development shall be done for the last application as it is closest to our current research [6] and [7].

The model structure is indicated in Fig. 1. Whether the links between particular systems - the agents - are physical (by means of springs or dashpots, for instance) or not (control laws for the platooning vehicles), is not a primary concern for the presented results. In case all agents are identical, a homogenous multi-agent model is obtained, representing e.g. a homogenous flexible beam or plate or a platoon composed of identical vehicles controlled by identical local controllers. Such dynamical systems are certainly strongly structured and important results based on symmetry can be obtained for them.

It is usually assumed that the measurement of the system outputs is not available. For such a case, the feedforward input shaping of the signal is the best option. Yet there are cases, for instance the vehicular platoons, where the measurement of the system is available. A feedback controller is then a natural candidate in the control design, since it can significantly improve the disturbance rejection of the system. However, the feedback controller does not guarantee the vibration-free excitation, see [6], which arises the following question. How can the feedforward input shaper be reformulated such that it makes use of the system measurement and yet it does not excite the oscillatory system poles? We answer the question in this paper.

A. Zero vibration (ZV) input shaping

Delay-based signal shapers are used today typically as reference command filters for manipulators with flexible or oscillatory load. The reference command for the manipulator is shaped by the shaper in such a way that the targeted oscillatory mode of the attached load is not excited. These ideas can be traced back to the 1950's when O. J. Smith published his PosiCast [8], known today more as the ZV shaper. In the 1990's, the subject was extensively studied by Singer and Seering [9]. They developed the original Smith's idea and proposed the concepts of zero-vibration (ZV), zero-vibration-derivative (ZVD) and extra insensitive (EI) shapers. The multi-mode shapers tuned to two or more selected flexible modes simultaneously that are utilized extensively in this paper were proposed in [10], [11], [12] and [13]. Among possible extensions of the ZV shaper is the DZV shaper, see [14], [15] and [16]. Input shapers have proved most useful in many application projects related to controls for oscillatory devices like flexible manipulators and cranes [17], industrial robots [18], solar panels of satellites [19], to name a few.

B. Wave-based control concept

The control of flexible structures such as beams and plates from by a travelling wave approach has its roots in 1960's, see [20] for one of the first treatment. It was followed by the Fourier-based spatial-transfer-function description in [21]. Not a long ago, the transfer function approach has been revisited in terms of an infinite dimensional transfer functions in a series of papers by Halevi in [22] and by O'Connor in [23] and [24]. The former introduced the *absolute vibration suppression* for control of continuous flexible mechanical structures, the latter proposed the *wave-based control* for positioning of a lumped flexible mechanical systems. Both the absolute vibration suppression and wave-based control are feedback controllers implemented on one or both structural ends with the task to absorb the incident travelling wave and thus reduce undesired system oscillations. Recently, the wave-based control has been generalized, under the name *wave-absorbing control*, even for a mechanically unconnected lumped models such as platoon of vehicles,

All authors are with the Czech Technical University in Prague. E-mail: martinec.dan@fel.cvut.cz

The research was supported by the Czech Science Foundation within the project No. 13-12726J. The contribution of M. Hromcik and T. Vyhlidal was supported by the Czech Science Foundation under the project No. 13-06962S. I. Herman was supported by the Czech Science Foundation within the project No. 13-06894S.

where the connection between the vehicles is created by controllers onboard each vehicle, see [6] and [7].

This paper treats a relation between the ZV shapers and the wave-absorbing controller. A similar comparison was conducted in [25] for absolute vibration suppression, wave-based control and a very simple version of an input shaper. We extend it by assuming a complex version of the input shaper, the multi-mode ZV (MMZV) shaper. We show that the impulse response of the MMZV shaper for the case when there are two integrators in the model of each agent converges to a double bell-shaped function. This finding allows us to design a control laws that combines the MMZV shaper and wave-absorbing controller in such a way that it does not excite the oscillatory system poles and yet it has a feedback part for absorption of the waves. Although the presented results are mostly based on the numerical simulations, they reveal a close connection between the input shaping and the travelling waves.

II. PRELIMINARIES

A. Local control law

We assume a chain of identical agents connected either mechanically or virtually by a controller onboard each agent. The agent indexed by n is modelled in the Laplace domain as

$$X_n(s) = P(s)U_n(s), \tag{1}$$

where s is the Laplace variable, $X_n(s)$ is the state of the agent, for instance the position, $P(s)$ is the transfer function of the model dynamics and $U_n(s)$ is the input to the agent. The input is generated by the connection with the neighbouring agents with the task to reach consensus on the states of all the agents.

Except of the agent, indexed $n = 0$, and the agent, indexed $n = N$, each agent has two neighbours, giving

$$U_n(s) = C(s)(X_{n-1}(s) - 2X_n(s) + X_{n+1}(s)). \tag{2}$$

We denote $M(s) = P(s)C(s)$, then the resulting model of the nth agent, see Fig. 1, is

$$X_n(s) = M(s)(X_{n-1}(s) - 2X_n(s) + X_{n+1}(s)). \tag{3}$$

The 0th agent, the so-called leader, is described as

$$X_0(s) = X_{\text{ref}}(s), \tag{4}$$

where $X_{\text{ref}}(s)$ is the desired steady state. The last agent of the chain is described as

$$X_N(s) = M(s)(X_{N-1}(s) - X_N(s)). \tag{5}$$

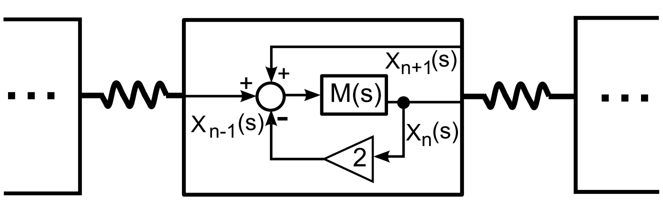

Fig. 1. The detail of the nth agent.

All the numerical simulations are carried out for $M(s) = (k_p s + k_i)/(s^3 + \xi s^2)$. Such a model is often used in theoretical studies, for instance, it represents a vehicle modelled by a double integrator with a linear model of damping, ξ, and controlled by a PI controller. In such a case, the state $X_n(s)$ represents the position of the nth vehicle. The two integrators in the open-loop model is, by the internal model principle, necessary for tracking a ramp signal in $X_0(s)$.

B. ZV input shaper

Consider the objective to compensate a single oscillatory mode of a system $H(s) = y(s)/v(s)$ represented by the natural frequency ω_0 and the damping ratio ζ, determining the complex conjugate couple of system poles $r_{1,2} = -\beta \pm \jmath\Omega, \beta = \omega_0\zeta, \Omega = \omega_0\sqrt{1-\zeta^2}$. For the oscillatory mode compensation purpose, we can use the simple ZV shaper [26], [9],

$$v(t) = \Lambda w(t) + (1-\Lambda)w(t-T), \tag{6}$$

where w and v are the shaper input and output, respectively. The parameters are the gain $\Lambda \in [0.5, 1]$ and the time delay $T \in \mathbb{R}^+$. The only dynamical element in the shaper is the time delay.

The zeros of shaper (6) are determined by the roots of the equation

$$S_{ZV}(s) = \Lambda + (1-\Lambda)e^{-sT} = 0, \tag{7}$$

which are given as follows

$$s_{2k+1,2k+2} = -\frac{1}{T}\ln\frac{\Lambda}{\Lambda-1} \pm \jmath\frac{\pi}{T}(2k+1), \tag{8}$$

where $k = 0, 1, ..., \infty$. From these infinitely many zeros, only the dominant pair $s_{1,2} = -(1/T)\ln(\Lambda/(\Lambda-1)) \pm \jmath\pi/T$ is used in fact to compensate the pole of the system $r_{1,2}$ [8], [27]. Placing the dominant zero $s_{1,2}$ of (6) at the position of $r_{1,2}$, the parameters of the shaper are given as follows

$$\Lambda = \frac{\exp(\pi\beta/\Omega)}{1+\exp(\pi\beta/\Omega)}, T = \frac{\pi}{\Omega} = \frac{\pi}{\omega_0\sqrt{1-\zeta^2}}. \tag{9}$$

C. Wave-based control

This paper is closely related to the research treated in [6], where the wave propagation in a platoon of identical vehicles is described. We briefly summarize the main idea of the paper.

The state of the nth agent in a chain of identical agents is composed of two parts, $A_n(s)$ and $B_n(s)$, that represent two waves propagating along the chain in the forward and backward directions, respectively. The mathematical model of a chain with infinitely many agents is

$$X_n(s) = A_n(s) + B_n(s), \tag{10}$$

$$A_{n+1}(s) = G(s)A_n(s), \tag{11}$$

$$B_n(s) = G^{-1}(s)B_{n-1}(s), \tag{12}$$

where the *wave transfer function*, $G(s)$, describes the wave propagation between two consecutive agents,

$$G(s) = \frac{1}{2}\alpha(s) - \frac{1}{2}\sqrt{\alpha^2(s)-4}, \tag{13}$$

$$G^{-1}(s) = \frac{1}{2}\alpha(s) + \frac{1}{2}\sqrt{\alpha^2(s)-4}, \tag{14}$$

with $\alpha(s) = 2 + 1/M(s)$. A mathematical model of a finite chain requires us to add wave reflections from the first and last agent in the chain, the so-called forced and free ends, which can again be described in terms of the wave transfer [6].

Both of the chain ends can be equipped with a wave-absorbing controller to prevent a reflection of the incident wave. The controller absorbs the wave by calculating the incident part of the wave and adding this part as a reference to its own local controller. Let us point out that, unlike the ZV input shaper, the wave-absorbing controller requires to measure the state of if immediate neighbour. In this paper, we assume that only the leader is equipped with the wave-absorbing controller, then

$$X_0 = X_{\text{ref}} + GB_1 = GX_1 + (1 - G^2)X_{\text{ref}}. \quad (15)$$

III. Characteristics of the MMZV shaper

The MMZV shaper is a series of ZV shapers, each designed for compensation of a single oscillatory mode of a system. Therefore, the MMZV shaper is described as,

$$F_{\text{MMZV}}(s) = \prod_{i \in \mathcal{P}} \left[\Lambda_i + (1 - \Lambda_i)\exp(-sT_i)\right], \quad (16)$$

where

$$\Lambda_i = \frac{\exp(\pi\beta_i/\Omega_i)}{1 + \exp(\pi\beta_i/\Omega_i)}, \quad T_i = \frac{\pi}{\Omega_i}, \quad (17)$$

$\beta_i = -\text{Re}(p_i)$, $\Omega_i = \text{Im}(p_i)$, $\mathcal{P}$ is a set of all complex poles of $T_{0,1}(s)$ with imaginary part greater than zero and p is a complex pole. We denote $f(t)$ as the impulse response of $F_{\text{MMZV}}(s)$.

The mathematical simulations of the impulse response of $F_{\text{MMZV}}(s)$ show that it converges to a double bell-shaped function, where we denote the time of the saddle point as τ_s. Fig. 2 shows impulse responses of $F_{\text{MMZV}}(s)$ for increasing number of agents, N. The top panel shows the impulse response as a function of time. The bottom panel shows the impulse response scaled in time such that the saddle points are centered at 1 on the x-axis. We can see that the τ_s grows and the maximum value of f decreases with the increasing N, see also Fig. 3, which shows that τ_s scales nearly linearly with N.

Analogously to (8), the zeros of the $F_{\text{MMZV}}(s)$ are calculated as

$$z_{i,k} = -\frac{1}{T_i}\ln\left(\frac{\Lambda_i}{\Lambda_i - 1}\right) + \frac{2k\pi\jmath}{T_i}, \quad i \in \mathcal{P}, \quad (18)$$

where $k \in \mathbb{Z}$. The zeros of $F_{\text{MMZV}}(s)$ and poles of $T_{0,1}(s)$ are shown in Fig. 4. We can see that some of the infinitely many zeros of the MMZV shaper are placed exactly on the oscillatory poles of $T_{0,1}(s)$. In fact, the zeros and poles coincide for $k \in \{0, 1\}$.

IV. Characteristics of the wave-based shaper

We reformulate the wave-absorbing controller as a feedforward input shaper, the *wave-based shaper*, to compare the wave-absorbing controller and the MMZV shaper. The wave-based shaper is designed such that the transfer function from $X_{\text{ref}}(s)$ to $X_1(s)$ is the same as for the wave-absorbing controller.

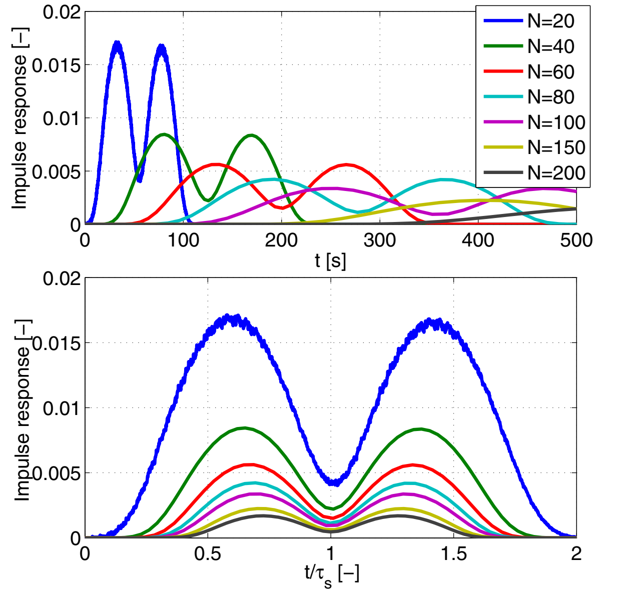

Fig. 2. The double bell-shaped impulse responses of the MMZV shaper shown for various values of N evaluated for $k_p = k_i = 1$, $\xi = 1.2$.

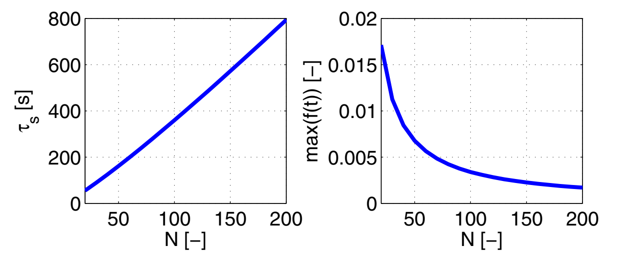

Fig. 3. Scaling of the time of the saddle point and the maximum value of the impulse response of $F_{\text{MMZV}}(s)$ with increasing N.

A. Mathematical definition

First, we find the transfer function from $X_0(s)$ to $X_1(s)$ in terms of the wave transfer function $G(s)$. From (10) we can write $X_1 = A_1 + B_1$. When the leader changes its state, it initiates a wave that propagates along the chain and reflects on both platoon ends. Hence, $A_1 = GX_0 - G^{2N+1}A_1$, $B_1 = G^{2N}X_0 - G^{2N+1}B_1$ and

$$T_{0,1}(s) = \frac{X_1(s)}{X_0(s)} = \frac{G(s)(1 + G^{2N-1}(s))}{1 + G^{2N+1}(s)}, \quad (19)$$

where $X_0(s)$ is the state of the leader from (15). Due to the wave-absorbing controller $A_1 = GX_0$ and $B_1 = G^{2N}X_0$. Hence,

$$T_{\text{WB}}(s) = \frac{X_1(s)}{X_{\text{ref}}(s)} = G(s)(1 + G^{2N-1}(s)). \quad (20)$$

Second, we introduce a feedforward filter $F_{\text{WB}}(s)$ for the leader with no wave-absorbing controller such that

$$X_0(s) = F_{\text{WB}}(s)X_{\text{ref}}(s). \quad (21)$$

From comparison of (19) and (20), we can see that if

$$F_{\text{WB}}(s) = 1 + G^{2N+1}(s), \quad (22)$$

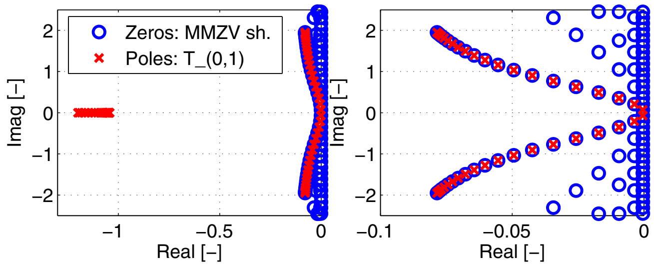

Fig. 4. The locations of the MMZV shaper zeros and $T_{0,1}(s)$ poles evaluated for $k_p = k_i = 1$, $\xi = 1.2$ and $N = 20$.

then the transfer function from $X_{\text{ref}}(s)$ to $X_1(s)$ is the same as in (20). The transfer function $F_{\text{WB}}(s)$ represents the wave-based shaper.

B. Zeros of the wave-based shaper

The zeros, z_i, of the wave-based shaper are solutions of the following equation

$$M(z_i) = \frac{1}{2(\cos(\pi L) - 1)}, \tag{23}$$

where $L = k/(2N+1)$ and $k = \{1, 3, 5, ..., 2N+1\}$. The proof is given in Appendix A.

We can see in Fig. 5 that all poles of $T_{0,1}(s)$, even the real ones, are covered by the wave-based shaper zeros, which is in agreement with (20). Besides zeros located on poles of $T_{0,1}(s)$, the wave-based shaper has also zeros resulting from the transfer function $(1 + G(s))$. This is due to the fact that $(1 + G(s))$ can be factored out from both the numerator and denominator of (19).

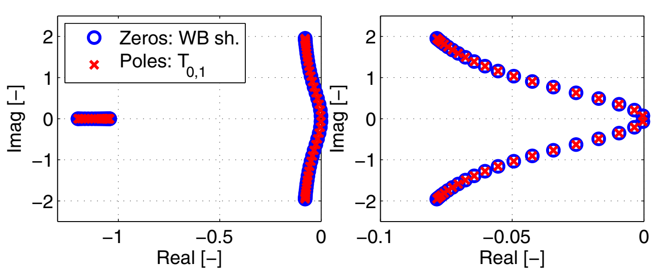

Fig. 5. The locations of the wave-based shaper zeros and $T_{0,1}(s)$ poles evaluated for $k_p = k_i = 1$, $\xi = 1.2$ and $N = 20$.

C. Performance of the wave-based shaper

Unlike the MMZV shaper, the wave-based shaper may excite the oscillatory poles of the system, which results in undesirable oscillation of the system. The comparison of responses of the system with high and low damping is shown in Fig. 6.

The settling time of the wave-based shaper grows better than linearly with the increasing N. The proof is the same as for the platoon with the wave-absorbing controller in [6]. We can see from Fig. 3, that the settling time of the MMZV shaper grows linearly as well. However, based on the simulation in Fig. 7, we can say that the transient is shorter for the wave-based shaper.

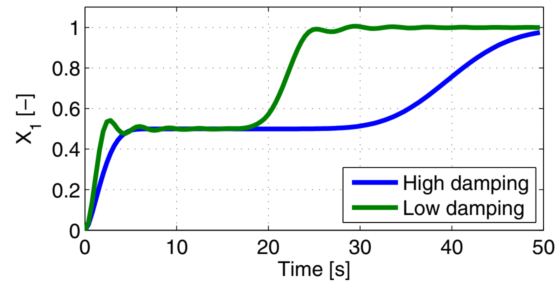

Fig. 6. The responses of the first agent with a wave-based shaper implemented on the leader. The simulation is performed for $N = 10$ with parameters $k_p = k_i = 1$. High and low damping is represented by $\xi = 4$ and $\xi = 1.2$, respectively.

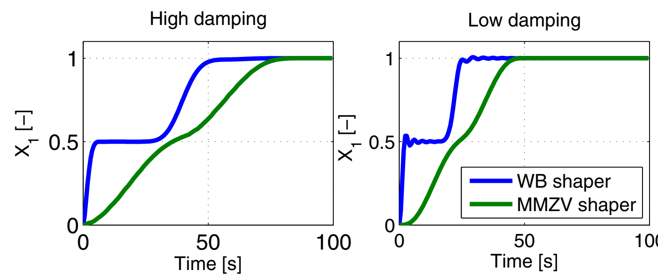

Fig. 7. The comparison of step responses of the first agent with the wave-based and MMZV shapers for $N = 10$. The model parameters are the same as in Fig. 6.

V. COMBINATION OF MMZV AND WAVE-BASED SHAPERS

A. Reduced MMZV shaper

The mathematical simulations show that the impulse response of the MMZV shaper can be composed of a two bell-shaped functions, $\overline{f}_{\text{a}}(t)$ and $\overline{f}_{\text{b}}(t)$. Mathematically,

$$f(t) = \overline{f}_{\text{a}}(t) + \overline{f}_{\text{b}}(t), \tag{24}$$

where

$$\overline{f}_{\text{b}}(t) \approx \overline{f}_{\text{a}}(t + \psi), \tag{25}$$

$\psi = 2(\tau_{\text{s}} - \tau_{\text{p}})$ and τ_{p} is the time of the first local maximum of $f(t)$ ($\tau_{\text{p}} = 80\,\text{s}$ in Fig. 8). The $\overline{f}_{\text{a}}(t)$ is obtained by taking the first part of the two bell-shaped function, $\overline{f}_{\text{a},1}(t_1)$, $t_1 \in [0, \tau_{\text{p}}]$, which is represented by the green line in Fig. 8, flipping it with respect to time and shifting it in time by τ_{p}. Mathematically,

$$\overline{f}_{\text{a}}(t_{\text{a}}) = \overline{f}_{\text{a},1}(t_1) \cup \overline{f}_{\text{a},2}(t_2), \tag{26}$$

$$\overline{f}_{\text{a},2}(t_2) = \overline{f}_{\text{a},1}(-t_1 + \tau_{\text{p}}), \tag{27}$$

where $t_{\text{a}} \in [t_1 \cup t_2]$, $t_1 \in [0, \tau_{\text{p}}]$, $t_2 \in [\tau_{\text{p}}, 2\tau_{\text{p}}]$.

We measure the convergence rate of $\overline{f}_{\text{a}}(t + \psi)$ to $\overline{f}_{\text{b}}(t)$ with the mean squared error (MSE) calculated as

$$\text{MSE}(\overline{f}_{\text{a}}(t + \psi)) = \frac{1}{T_{\text{end}}} \sum_{t=0}^{T_{\text{end}}} \left[\overline{f}_{\text{a}}(t + \psi) - (f(t) - \overline{f}_{\text{a}}(t)) \right]^2, \tag{28}$$

where T_{end} is the simulation time, in our case $T_{\text{end}} = 500\,s$, with the time step $T_{\text{step}} = 0.05\,s$. We can see in Fig. 11, that

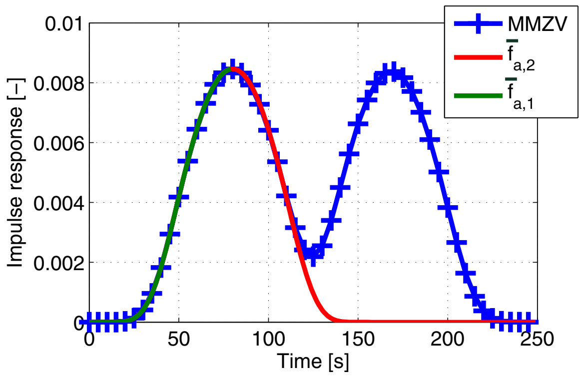

Fig. 8. The comparison of $f(t)$, $\overline{f}_{a,1}(t_1)$ and $\overline{f}_{a,2}(t_2)$ for $k_p = k_i = 1$, $\xi = 1.2$ and $N = 40$. The impulse response of the MMZV shaper, $f(t)$, is represented the blue-plus line. The green and red lines stand for $\overline{f}_{a,1}(t_1)$ and $\overline{f}_{a,2}(t_2)$, respectively. The composition of the green and red lines gives $\overline{f}_{\mathrm{a}}(t)$.

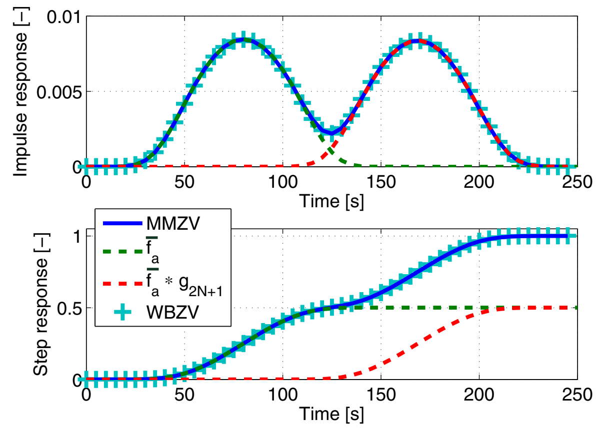

Fig. 9. Step and impulse responses of MMZV and WBZV shapers. The model parameters are the same as in Fig. 8.

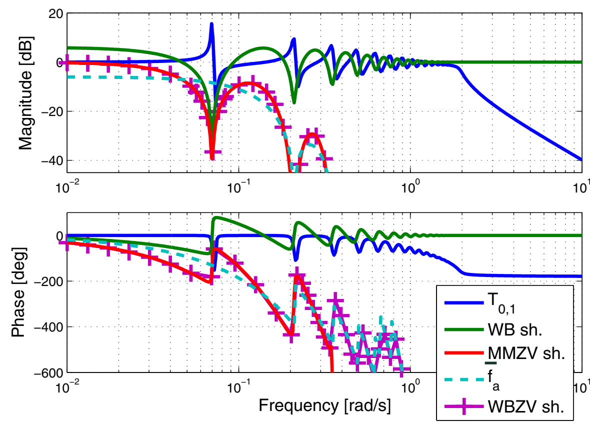

Fig. 10. Frequency characteristics of MMZV and WBZV shapers. The model parameters are the same as in Fig. 8.

the convergence rate is almost exponential, regardless of the model damping.

B. Wave-based MMZV (WBZV) shaper

The WBZV shaper is the combination of the MMZV shaper and the wave-based shaper. The key idea is to replace the time shift ψ by a convolution such that

$$\overline{f}_{\mathrm{b}}(t) \approx \overline{f}_{\mathrm{a}}(t) * g_{2N+1}(t), \tag{29}$$

where $g_{2N+1}(t)$ is the impulse response of $G^{2N+1}(s)$. The impulse response of the WBZV is then

$$h(t) = \overline{f}_{\mathrm{a}}(t) * (\delta(t) + g_{2N+1}(t)), \tag{30}$$

where $\delta(t)$ is the Dirac delta function.

From comparison of the impulse and step responses in Fig. 9 and the frequency response in Fig. 10, we can see that

$$f(t) \approx h(t). \tag{31}$$

The convergence rate of $h(t)$ to $f(t)$ is measured with the MSE calculated as

$$\mathrm{MSE}(h(t)) = \frac{1}{T_{\mathrm{end}}} \sum_{t=0}^{T_{\mathrm{end}}} (h(t) - g(t))^2 . \tag{32}$$

Fig. 11 shows that the convergence rate is almost exponential, regardless of the model damping.

VI. Discussion of the Results

We have shown that the WBZV shaper is almost identical to the MMZV shaper. The advantage of the WBZV shaper is that it can be reformulated as a combination of a feedforward and feedback controller as follows. The WBZV shaper is composed of two input shapers connected in series with the impulse responses $\overline{f}_{\mathrm{a}}(t)$ and $(\delta(t) + g_{2N+1}(t))$, respectively. The latter is the impulse response of the wave-based shaper from (22), which was obtained by reformulation of the wave-absorbing controller in terms of a feedforward shaper. Therefore, the control law with the feedforward shaper, defined by $\overline{f}_{\mathrm{a}}(t)$, and wave-absorbing controller implemented on the leader has the same impulse response as the WBZV shaper and almost the same as the MMZV shaper. This means that such a control law does not excite the oscillatory poles, unlike WB shaper, moreover, it has a better rejection of the disturbance acting in the system due to the feedback part from the wave-absorbing controller. The proposed control law is summarized in Fig. 12.

Eq. (31) shows yet another, the travelling-wave, interpretation of the MMZV shaper. First, the actuator initiates the travelling wave without exciting the oscillatory poles, which is represented by $\overline{f}_{\mathrm{a}}(t)$. Then the actuator let the wave to propagate to the opposite chain end where the wave reflects and returns back to the actuated end. When the wave reaches the actuated end, the actuator absorbs it by adding $\overline{f}_{\mathrm{a}}(t) * g_{2N+1}(t)$ to its state.

VII. Conclusions

The paper shows a connection between the multi-mode zero vibration shaper and the wave absorbing controller for a chain of multi-agent dynamical systems with two integrators in the model of each agent. The two control approaches can be brought together for design of the control law that

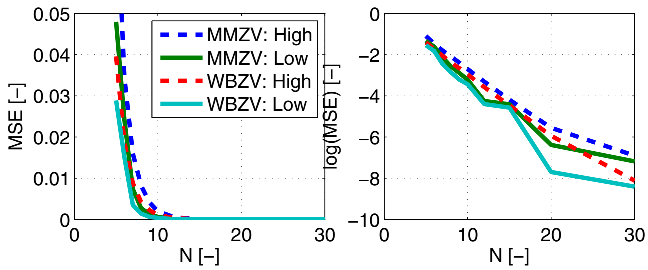

Fig. 11. Convergence rates of the reduced MMZV and WBZV shapers evaluated with MSE measures from (28) and (32), respectively. The labels 'High' and 'Low' stand for the high and low damping, respectively. The model parameters are the same as in Fig. 6.

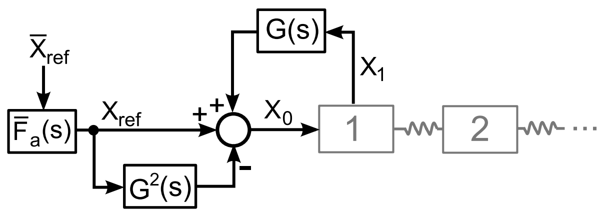

Fig. 12. The control law combining the MMZV shaper and the wave-absorbing controller, where $\overline{F}_\mathrm{a}(s)$ is the Laplace transform of $\overline{f}_\mathrm{a}(t)$.

combines the zero-vibration excitation of the system with the feedback absorption of the travelling waves on the chain ends. The presented preliminary results are mostly based on the numerical simulations. The analytic proofs are subject of the future study.

Appendix

A. Proof of zeros of the wave-based shaper

The zeros of the wave-based shaper are solutions of the equation $G^{2N+1}+1=0$, or, equivalently,

$$G=(-1)^{1/(2N+1)}. \tag{33}$$

The substitution from (13) for G and $\exp(\pi \jmath)$ for -1 gives

$$\frac{1}{2}\alpha-\frac{1}{2}\sqrt{\alpha^2-4}=\exp(\pi \jmath L), \tag{34}$$

where $L=k/(2N+1)$ and $k=\{1,3,5,...,2N+1\}$. Simplification of (34) yields

$$\alpha=\exp(\pi jL)+\exp(-\pi jL)=2\cos(\pi L). \tag{35}$$

Finally, substituting $\alpha=2+1/M$ gives

$$M(z_i)=\frac{1}{2(\cos(\pi L)-1)}, \tag{36}$$

where z_i are zeros of the wave-based shaper.

References

[1] S. K. Dwivedy and P. Eberhard, "Dynamic analysis of flexible manipulators, a literature review," *Mechanism and Machine Theory*, vol. 41, no. 7, pp. 749–777, July 2006.

[2] T. Dhaene and D. D. Zutter, "Selection of lumped element models for coupled lossy transmission lines," *Computer-Aided Design of Integrated . . .*, no. July, pp. 805–815, 1992.

[3] P. Seiler, A. Pant, and K. Hedrick, "Disturbance Propagation in Vehicle Strings," *IEEE Transactions on Automatic Control*, vol. 49, no. 10, pp. 1835–1841, Oct. 2004.

[4] D. Swaroop and J. K. Hedrick, "Constant Spacing Strategies for Platooning in Automated Highway Systems," *Journal of Dynamic Systems, Measurement, and Control*, vol. 121, no. 3, p. 462, 1999.

[5] J. Eyre, D. Yanakiev, and I. Kanellakopoulos, "A Simplified Framework for String Stability Analysis of Automated Vehicles∗," *Vehicle System Dynamics*, 1998.

[6] D. Martinec, I. Herman, Z. Hurák, and M. Šebek, "Wave-absorbing vehicular platoon controller," *European Journal of Control*, vol. 20, pp. 237–248, 2014.

[7] D. Martinec, I. Herman, and M. Sebek, "Two-sided wave-absorbing control of a heterogenous vehicular platoon," in *Proceedings of the 19th IFAC World Congress, 2014*, no. 1986, 2014, pp. 8091–8096.

[8] O. Smith, "Posicast control of damped oscillatory systems," *Proceedings of the IRE*, pp. 1249–1255, 1957.

[9] W. Singhose, W. Seering, and N. Singer, "Residual vibration reduction using vector diagrams to generace shaped inputs," *Journal of Mechanical Design*, vol. 116, pp. 654–659, 1994.

[10] Y. Sung and W. Singhose, "Robustness analysis of input shaping commands for two-mode flexible systems," *Control Theory and Applications, IET*, vol. 3, no. 6, pp. 722–730, 2009.

[11] T. Tuttle and W. Seering, "A zero-placement technique for designing shaped inputs to suppress multiple-mode vibration," *American Control Conference, 1994*, vol. 3, pp. 2533–2537, 1994.

[12] J. Hyde and W. Seering, "Using input command pre-shaping to suppress multiple mode vibration," *Robotics and Automation IEEE Conference, 1991.*, pp. 2604–2609, 1991.

[13] T. Singh and S. Vadali, "Robust time-delay control of multimode systems," *International Journal of Control*, vol. 62, pp. 1319–1339, 1995.

[14] T. Vyhlídal, V. Kučera, and M. Hromčík, "Signal shaper with a distributed delay: Spectral analysis and design," *Automatica*, vol. 49, no. 11, pp. 3484–3489, Nov. 2013.

[15] T. Vyhlidal, V. Kucera, and M. Hromcik, "Input shapers with uniformly distributed delays," *10th IFAC Workshop in Time Delay Systems*, pp. 91–96, 2012.

[16] ——, "Zero vibration shapers with distributed delays of various types," in *52nd IEEE Conference on Decision and Control*. IEEE, Dec. 2013, pp. 940–945.

[17] D. Kim and W. Singhose, "Performance studies of human operators driving double-pendulum bridge cranes," *Control Engineering Practice*, vol. 18, no. 6, pp. 567–576, 2010.

[18] E. Pereira, J. Trapero, I. Díaz, and V. Feliu, "Adaptive input shaping for manoeuvring flexible structures using an algebraic identification technique," *Automatica*, vol. 45, no. 4, pp. 1046–1051, 2009.

[19] W. Singhose, S. Derezinski, and N. Singer, "Extra-insensitive input shapers for controlling flexible spacecraft," *Journal of Guidance, Control, and Dynamics*, vol. 19, pp. 285–391, 1996.

[20] D. R. Vaughan, "Application of Distributed Parameter Concepts to Dynamic Analysis and Control of Bending Vibrations," *Journal of Basic Engineering*, vol. 90, no. 2, pp. 157–166, June 1968.

[21] A. H. Flotow, "Disturbance propagation in structural networks," *Journal of Sound and Vibration*, vol. 106, no. 3, pp. 433–450, 1986.

[22] Y. Halevi, "Control of Flexible Structures Governed by the Wave Equation Using Infinite Dimensional Transfer Functions," *Journal of Dynamic Systems, Measurement, and Control*, vol. 127, no. 4, p. 579, 2005.

[23] W. J. O'Connor, "Wave-echo control of lumped flexible systems," *Journal of Sound and Vibration*, vol. 298, no. 4-5, pp. 1001–1018, Dec. 2006.

[24] ——, "Wave-Based Analysis and Control of Lump-Modeled Flexible Robots," *IEEE Transactions on Robotics*, vol. 23, no. 2, pp. 342–352, Apr. 2007.

[25] I. Peled, W. O'Connor, and Y. Halevi, "On the relationship between wave based control, absolute vibration suppression and input shaping," *Mechanical Systems and Signal Processing*, pp. 1–11, June 2012.

[26] N. Singer and W. Seering, "Preshaping command inputs to reduce system vibration," *Journal of Dynamics, System, Measure and Control*, vol. 112, pp. 76–82, 1990.

[27] J. Huey and W. Singhose, "Trends in the stability properties of CLSS controllers: a root-locus analysis," *IEEE Transactions on control system technology*, vol. 18, pp. 1044–1056, 2010.